Acta Cryst. (1995). D**51**, 805–813

Refined Structure of Cu-Substituted Alcohol Dehydrogenase at 2.1 Å Resolution

BY SALAM AL-KARADAGHI* AND EILA S. CEDERGREN-ZEPPEZAUER†

Department of Structural Chemistry, Arrhenius Laboratories for Natural Sciences, Stockholm University, S-106 91 Stockholm, Sweden

AND ZBIGNIEW DAUTER AND KEITH S. WILSON

European Molecular Biology Laboratory (EMBL), c/o DESY, Notkestrasse 85, D-22603 Hamburg, Germany

(*Received* 8 *March* 1994; *accepted* 9 *January* 1995)

Abstract

Liver alcohol dehydrogenase (LADH) is a Zn^{II}-dependent dimeric enzyme. LADH with the active-site Zn^{II} substituted by Cu^{II} resembles blue (type I) copper proteins by its spectroscopic characteristics. In this work we present the X-ray structure of the active site Cu^{II}-substituted LADH complex with NADH and dimethyl sulfoxide (DMSO). The structure was solved by molecular replacement. The space group is $P2_1$ with cell dimensions $a = 44.4$, $b = 180.6$, $c = 50.8$ Å and $\beta = 108°$. There is one dimer of the enzyme in the asymmetric unit. The refinement was carried out to a crystallographic R factor of 16.1% for 41 119 unique reflections in the resolution range 12.0 to 2.1 Å. The coordination geometry of Cu^{II} in LADH is compared with the active-site metal coordination in the Zn–LADH–NADH–DMSO complex and blue-copper proteins. The distances from the metal to the protein ligands (Cys46, His67 and Cys174) are similar for the Zn^{II} and Cu^{II} ions. The distances of the O atom of the inhibitor DMSO to the Cu^{II} ion in the two subunits of the dimer are 3.19 and 3.45 Å. These are considerably longer than the corresponding distances for the Zn^{II} enzyme, 2.19 and 2.15 Å. The Cu^{II} ion is positioned nearly in the plane of the three protein ligands (NS_2) with a geometry similar to the trigonal arrangement of the three strongly bound ligands (N_2S) in blue-copper proteins. This coordination probably accounts for the similarity of the spectral characteristics of Cu^{II}–LADH and type I copper proteins.

Introduction

Liver alcohol dehydrogenase (LADH) belongs to a large family of nucleotide-binding proteins. The enzyme reversibly catalyses the oxidation of various alcohols to the corresponding aldehydes and ketones. The oxidation of the alcohol group of the substrate occurs by a transfer of a hydride ion from the C1 atom that carries the hydroxyl group to the C4 atom of the oxidized form of NAD. In addition a proton is removed from the alcohol hydroxyl group. The kinetics of the reaction are described by the Theorell–Chance compulsory binding order mechanism (Theorell & Chance, 1951; Brändén, Jörnvall, Eklund & Furugren, 1975).

LADH is a dimer of two identical subunits each consisting of 374 amino acids. Each subunit binds one NAD molecule to the coenzyme-binding domain consisting of residues 176–318. It is folded into a classical α/β unit with a central six-stranded β-pleated sheet flanked by five α-helices forming the connection between the strands. Two Zn^{II} ions are bound to each catalytic domain (residues 1–175 and 319–374). The majority of these residues are folded into a complex pattern of mainly antiparallel strands and four helical segments (Eklund *et al.*, 1976). The catalytic zinc ion is coordinated to three protein residues, Cys46, Cys174 and His67, the fourth ligand being a water molecule which can be replaced by a substrate or an inhibitor. The non-catalytic Zn^{II} is not involved directly in catalysis. It is liganded to cysteines 97, 100, 103 and 111 in a close to ideal tetrahedral geometry.

The catalytic site in LADH has been the subject of extensive studies by crystallographic and spectroscopic methods and by means of metal substitutions. The Zn^{II} ion has been found to participate in binding, orienting and polarizing the substrate, acting as a Lewis acid during the redox reaction (Eklund, Plapp, Samama & Brändén, 1982; Cedergren-Zeppezauer, Samama & Eklund, 1982; Dunn, Dietrich, MacGibbon, Koerber & Zeppezauer, 1982). From X-ray crystallographic studies it has been shown that in different conformational states of the enzyme the coordination geometry of the active-site zinc is invariably distorted tetrahedral (Eklund, Jones & Schneider, 1986; Al-Karadaghi *et al.*, 1994). This geometry is preserved after binding of the inhibitor dimethyl sulfoxide (DMSO) and the transition of the protein to the closed form in the presence of NADH (Eklund *et al.*, 1981; Al-Karadaghi *et al.*, 1994) and after substituting the active-site zinc by Co^{II} or Cd^{II} ions (Schneider, Eklund, Cedergren-Zeppezauer &

* Present address: Department of Molecular Biophysics, Lund University, PO Box 124, 221 00 Lund, Sweden.

† Author for correspondence.

ISSN 0907-4449

Zeppezauer, 1983; Schneider, Cedergren-Zeppezauer, Knight, Eklund & Zeppezauer, 1985).

Unlike Cd^{II}– and Co^{II}–LADH, the Cu^{II}-substituted enzyme was reported to be inactive (Maret, Dietrich, Ruf & Zeppezauer, 1980). However, it has been an attractive research object due to the similarity of its optical and EPR spectroscopic characteristics to those of blue (type I) copper proteins (cupredoxins). Cu^{II}–LADH exhibits an unusual (when compared to small-molecule Cu complexes) intense electronic absorption band near 620 nm (ε about 4000 M^{-1} cm^{-1}), an anomalously small hyperfine coupling constant in the EPR spectrum (Maret *et al.*, 1980, 1981, 1983; Maret, Zeppezauer, Sanders-Loehr & Loehr, 1983) and a resonance Raman spectrum characteristic of type I copper proteins (Maret *et al.*, 1986). Binding of coenzyme and active-site metal ligands affect the spectroscopic parameters of the Cu centre. Thus, NAD^+ and NADH cause large shifts of the absorption maximum at 620 nm to 650 and 690 nm, respectively (Maret *et al.*, 1980; Maret & Kozlowski, 1987). Low-temperature absorption spectra of the binary complexes with metal ligands pyrazole, imidazole, β-mercaptoethanol and cyanide are also shifted to about 500 nm from the 570 nm maximum. In the resonance Raman spectra the binding of these ligands causes significant shifts (3–20 cm^{-1}) in the four main Cu cysteinate vibrations, accompanied by substantial decrease in the intensity of the two high-energy peaks. For the crystalline ternary complex with NADH and DMSO (the structure of which is presented in this work) the electronic absorption maximum is centred at 665 nm (Merli, Rossi & Cedergren-Zeppezauer, unpublished results).

The structural basis for the interpretation of the spectroscopic properties of blue-copper proteins was provided by high-resolution X-ray crystallographic data. From the structures of plastocyanin (Guss & Freeman, 1983; Guss, Bartunik & Freeman, 1992) azurin (Baker, 1988; Nar *et al.*, 1992), pseudoazurin (Petratos, Dauter & Wilson, 1988; Adman *et al.*, 1989; Inoue *et al.*, 1994) and the cucumber basic blue protein (Guss *et al.*, 1988) the overall similarity of Cu^{II} coordination has been established. The Cu^{II} ion was found to be coordinated to two histidines and one cysteinate in a distorted trigonal geometry, with weakly ligated methionine S and carbonyl O atoms (in azurin) at longer distances. One of the characteristic features of these copper sites is the shortness of the Cu—S(Cys) bond. The average value from several structures is 2.12 Å with estimated uncertainties of 0.05 Å (Han *et al.*, 1991). Also the Cu^{II}–ligand dihedral angles and the hydrogen-bond network involving the ligands and the adjacent residues appear to be among the conserved features of blue-copper proteins.

Taking into account the relationship between coordination and spectral properties of Cu^{II} sites in blue-copper proteins, one would expect at least some similarities between the geometry of the Cu^{II} site in LADH and type I copper proteins. However, in LADH the metal ion is chelated by two cysteinates and from spectroscopic measurements alone it is impossible to separate their contribution to the spectral properties. Hence, an X-ray structure of Cu^{II}–LADH would provide a basis for the understanding of its spectral characteristics. This work has been hampered by difficulties associated with the crystallization of the Cu^{II}-substituted enzyme. Due to a relatively fast bleaching of the protein solution during exposure to atmospheric oxygen, the crystallization, which takes several weeks, has to be performed in a strictly oxygen-free environment (see *Materials and methods* section for details). This process was interpreted in terms of a reduction of Cu^{II} to Cu^{I}. However, the mechanism behind it remains unclear (some discussion is provided by Maret, Zeppezauer, Desideri, Morpurgo & Rotilio, 1983).

In this work we present the crystal structure of Cu^{II}-substituted LADH in complex with NADH and DMSO at 2.1 Å resolution. The coordinates have been deposited with the Protein Data Bank at Brookhaven.*

Materials and methods

Crystallization and data collection

The preparation of Cu^{II}-substituted LADH has been described earlier (Maret *et al.*, 1980). The starting material, microcrystalline active-site Zn^{II}-depleted enzyme, was a generous gift from Professor M. Zeppezauer, University of Saarbrücken, Germany. Crystallization of the reconstructed Cu^{II}-enzyme in complex with NADH and DMSO was performed in sealed glass vessels under suprapure nitrogen at 277 K. The inert atmosphere was necessary to protect the Cu^{II}-enzyme from oxygen, which causes bleaching of the blue colour of the crystals. A 2% protein solution was dialyzed against 0.75 m*M* NADH and 1.5%(*v*/*v*) DMSO in 0.05 *M* Tris–HCl buffer, pH 8.2. The precipitating agent, freshly distilled 2-methyl-2,4-pentanediol (MPD), was slowly added to the outer dialysis solution. At a concentration of 10% MPD small crystals started to appear. These were allowed to grow for one month with successive additions of precipitant to a final concentration of 20%. Crystals for X-ray analysis were mounted under nitrogen in glass capillaries using a glove box. The crystals belonged to space group $P2_1$ with cell dimensions $a = 44.4$, $b = 180.6$, $c = 50.8$ Å and $\beta = 108.0°$.

Three-dimensional data were collected from a single crystal at the EMBL X31 beamline at the DORIS storage

* Atomic coordinates and structure factors have been deposited with the Protein Data Bank, Brookhaven National Laboratory (Reference: 2OXI, R2OXISF). Free copies may be obtained through The Managing Editor, International Union of Crystallography, 5 Abbey Square, Chester CH1 2HU, England (Reference: GR0376).

ring, DESY, Hamburg. The ring was operating at 3.7 GeV and 40–90 mA with approximately 3 h between injections. The crystal was mounted on a φ-rotation axis from an Enraf–Nonius camera and cooled with a stream of air (277 K) during data collection. Data were recorded using an imaging-plate scanner designed and built at the EMBL outstation in Hamburg by J. Hendrix and colleagues. Two-dimensional images were transferred directly to a computer disk for subsequent analysis and integration of the diffraction patterns. During the collection of high-resolution data many of the strong low-resolution reflections were saturated. Due to this limitation of the dynamic range of the scanner, collection of one additional data set with different exposure times was necessary.

The images were evaluated with a modified version of the *MOSFLM* film-processing package (Leslie, Brick & Wonacott, 1986). Subsequent calculations were performed using the *CCP*4 programs (Collaborative Computational Project, Number 4, 1994) supplied by the SERC Daresbury Laboratory. The *ROTAVATA/AGROVATA* programs were used to merge the data and to extract the unique set of reflections. The program *TRUNCATE* (French & Wilson, 1978) was used to convert the intensities to structure-factor amplitudes. Details of the data collection are presented in Table 1.

Table 1. *Summary of data collection for the* Cu–*LADH–NADH–DMSO complex*

Space group	$P2_1$
Cell dimensions (Å, °)	$a = 44.4$, $b = 180.6$, $c = 50.8$, $\beta = 108$
No. of crystals used	1
Approx. dimensions (mm)	1 × 1 × 0.7
Wavelength of X-rays (Å)	1.009
Crystal-to-film distance (mm)	205 and 305
No. of images	
2.1–3.0 Å range	135
3.0–12.0 Å range	64
Total No. of measurements	81533
No. of unique reflections	41119
Resolution range (Å)	12.0–2.1
Completeness (%)	93.5
$R(I)_{merge}$*	0.044 (0.076 at 2.1 Å)
93.2% reflections had $I > \sigma$	
87.9% reflections had $I > 2\sigma$	
83.8% reflections had $I > 3\sigma$	
$\langle I \rangle / \sigma(I) = 8.4$ at 2.1 Å resolution.	

* $R(I)_{merge}$ is defined as $\sum |I_i - \langle I \rangle| / \sum I$, where I_i is an individual intensity measurement and $\langle I \rangle$ is the average intensity for this reflection.

Molecular replacement and refinement

The structure of Cu^{II}–LADH was solved by molecular replacement (Rossman & Blow, 1962) as implemented in the program system *X-PLOR* (Brünger, Karplus & Petsko, 1989; Brünger, 1990). The structure of native dimeric LADH (Zn^{II}–LADH) refined at 1.8 Å resolution (Al-Karadaghi *et al.*, 1994) to a crystallographic *R* factor of 17.3% was used as search model. First a rotation search was carried out in the resolution range 8.0–3.0 Å. The two highest peaks had correlation coefficients 0.40 and 0.35 and were related to each other by a rotation of 180°. This is an effect of the approximate twofold axis, which relates the two subunits of the enzyme. The orientation with the highest correlation coefficient was further refined utilizing the PC-refinement option in *X-PLOR*. After the refinement the correlation coefficient increased to 0.45. This orientation was used for the translation search. It was carried out in the resolution range 8.0–3.0 Å and the criterion used was the correlation coefficient between E^2_{obs} and E^2_{cal} (the squared amplitudes of the observed and calculated normalized structure factors). The translation vector with the highest value of the translation function (0.85) was applied to the rotated search model.

The rotated and translated model with all the solvent molecules included was subjected to rigid-body refinement using *X-PLOR*. Four independent units were refined: the coenzyme-binding domain, the catalytic domain, NADH and DMSO. During this and subsequent stages the two subunits of the dimer (denoted *A* and *B* in the text) were refined independently without applying symmetry restraints. The crystallographic *R* factor dropped from 35 to 31% after rigid-body refinement. The model was subjected to 120 cycles of restrained positional refinement in the resolution range 8.0–3.0 Å. This was followed by a gradual extension of resolution in 0.2 Å steps with 60 cycles of positional refinement at each step until the limit of the resolution of the data was reached, 2.1 Å. 15 cycles of restrained *B*-factor refinement brought the *R* factor to 20.2%.

During the refinement the positions of the four metal ions were constrained by a harmonic constant of 100 kcal mol^{-1} Å^{-2}, the liganding S atoms from Cys46, Cys174, Cys97, Cys100, Cys103, Cys111 and NE2 from His67 by 10 kcal mol^{-1} Å^{-2}. No restraints were imposed on the metal–ligand distances. The harmonic constant on the metal ions and their ligands were set to zero in the last cycles of the refinement to allow for a relaxation of the coordination sphere in order to obtain more accurate metal-binding parameters. The metal radius was artificially decreased to reduce metal–ligand repulsion.

An overall anisotropic temperature factor was calculated, refined and applied to the diffraction data. This caused a decrease of the *R* factor to 17.3% in the resolution range 12–2.1 Å. The respective coefficients of the atomic displacement factor U_{ij} ($B = 8\pi U$) were $U_{11} = 0.03$, $U_{22} = 0.12$, $U_{33} = -0.15$ and $U_{13} = 0.01$ Å^2.

Density maps with coefficients $2F_o - F_c$ and $F_o - F_c$ were calculated using the coordinates from the last step. The positions of all side chains and solvent molecules in both subunits were checked and rebuilt manually when necessary using the program system *FRODO* (Jones, 1978) implemented on an Evans & Sutherland PS300 graphics station. Only minor rebuilding of some surface side chains was necessary. This demonstrates the close

similarity of the three-dimensional structures of the ternary complexes of triclinic Zn^{II}–LADH and monoclinic Cu^{II}–LADH. All water molecules with *B* factors higher than 75 Å^2 were deleted from the model. The $F_o - F_c$ map was checked with the program *PEAKMAX* and about 50 new solvent molecules in both subunits were added to the model after checking for possible hydrogen bonds to protein groups and to other solvent sites. The model was subjected to 80 cycles of positional refinement followed by 15 cycles of isotropic *B*-factor refinement. The resulting *R* factor was 16.5%.

New density maps were calculated. Residues which had been rebuilt during the previous step were inspected. Side-chain atoms for which there was not any clear electron density were assigned zero occupancy (about 150 of the total of 5584 atoms). Similar to the Zn^{II}–LADH, the side chains of Cys281*A*, Cys282*A*, Cys282*B* were discretely disordered. However, no significant positive $F_o - F_c$ density could be observed in the vicinity of Cys281*B*. Strong positive peaks in the difference-density map were observed close to Cys46. One peak is directed towards the side chain of Glu68 approximately opposite to the Cu^{II} liganding position of Cys46 in both subunits of the dimer. This position of the S atom is reminiscent of that found in metal-depleted LADH (Schneider *et al.*, 1983) and indicates disorder due to a not fully occupied Cu^{II} site. Another peak was observed only in the *A* subunit in a position between Cys46 (1.68 Å to SG), the O1PN group of NADH (2.79 Å), the NH_2 group of Arg369 (2.70 Å) and at 3.4 Å from the metal site. Due to the short distance to SG46 this peak could not be interpreted as a solvent site, although O1PN and NH_2 are at hydrogen-bonding distance. However, in the Cu-free fraction of the enzyme there could be a water molecule at this site, since SG46 would be pointing towards another direction in this case.

The alternative conformations were generated and built manually into the electron density. The positions of the sulfur atoms were related by a torsional rotation around the C*A*—C*B* bond of 110° for Cys281*A*, and about 180° for Cys282 in both *A* and *B* subunits. The occupancy of these disordered side-chain atoms, of the two copper ions and the inhibitor DMSO were refined. The values for the second conformations of Cys281*A*, Cys282*A* and Cys282*B* were approximately 0.20. For the Cu^{II} and the liganding sulfur from Cys46 the values were about 0.7 and 0.8 in the *A* subunit, 0.6 and 0.8 in the *B* subunit, respectively. For the inhibitor DMSO a value of about 0.85 was obtained for both subunits.

During the last 40 cycles of the positional refinement the restraints on the metal ions and the liganding protein groups were released. After 15 cycles of individual isotropic *B*-factor refinement the final *R* factor was 16.1% with all the reflections in the resolution range 12.0–2.1 Å included. There were 446 solvent molecules. Further positional refinement did not lead to any improvement in the *R* factor.

Accuracy of the final model

The r.m.s. deviation from ideality for bond lengths was 0.019 Å and the respective values for bond angles and dihedral angles were 3.36 and 26.23°.

Figs. 1(*a*) and 1(*b*) present the *R* factor as a function of resolution and the σ_A plot (Read, 1986) for the final model. The upper limit of the coordinate error estimated from the σ_A plot is about 0.24 Å.

The Ramachandran plot (Ramachandran & Sasisekharan, 1968) showing the distribution of (φ, ψ) angles is presented on Figs. 2(*a*) and 2(*b*) for the *A* and *B* subunits, respectively. It is evident from the plot that the geometry of the model is of good quality. Residue Cys174 in both subunits has unusual (φ, ψ) values: (−156, −84°) in the *A* subunit and (−157, −73°) in the *B* subunit. Cys174, which chelates the active-site metal, is located at the top of a kink formed by Gly173 and Gly175 in the middle of a helix (residues Pro165–Val189). This conformation is essential for the coordination of the S atom to the metal

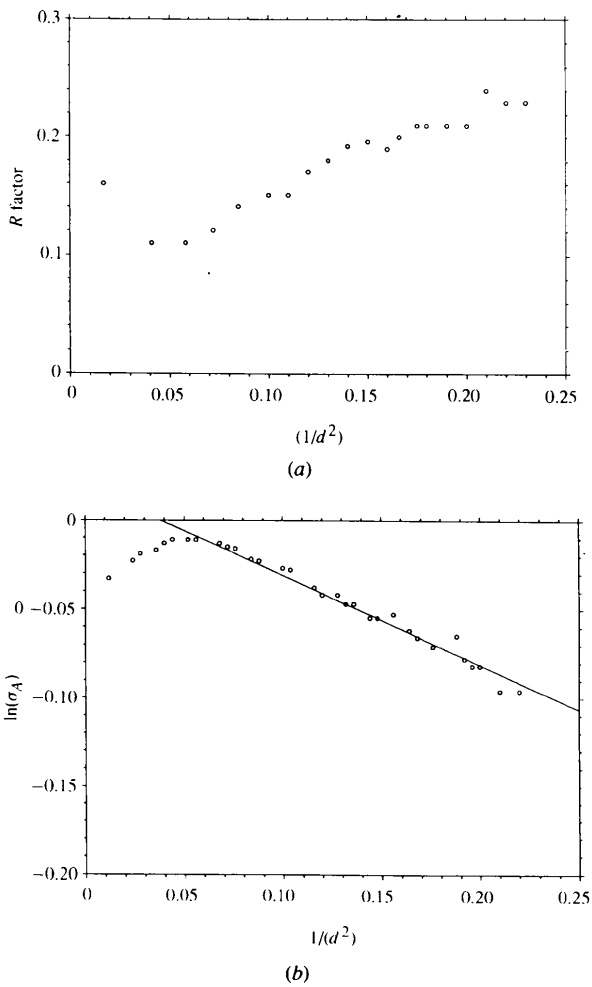

Fig. 1. The *R* factor as a function of resolution (*a*) and the σ_A plot (*b*) for Cu^{II}–LADH.

ion. Ile368 with torsion angles (−99, −89°) and (−101, −81°) in the *A* and *B* subunits, respectively, is positioned at a sharp corner before strand 2 (residues 369–374) of the sheet β-I (nomenclature is defined in the PDB entry). This conformation is stabilized by an extensive hydrogen-bonding network, which involves main- and side-chain atoms of the neighboring residues, solvent molecules and the coenzyme NADH (Al-Karadaghi *et al.*, 1994). The non-glycine residues in the left-handed helical region of the plot are associated with turns or with positions at C termini of α-helices. The same residues were found in the left-handed helical region in the triclinic native Zn–LADH–NADH–DMSO structure.

The average *B* factor for all the atoms is 28 Å^2 and after excluding solvent molecules 26.5 Å^2. The average *B* factor for the *A* subunit, 29 Å^2, is somewhat higher than the corresponding value for the *B* subunit, 24 Å^2.

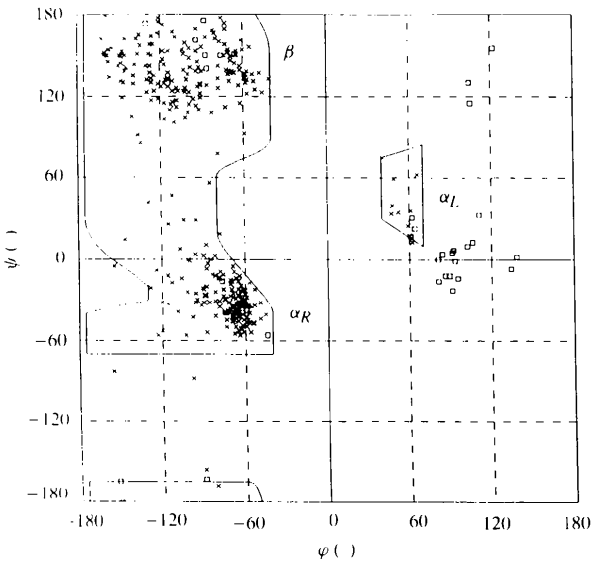

(*a*)

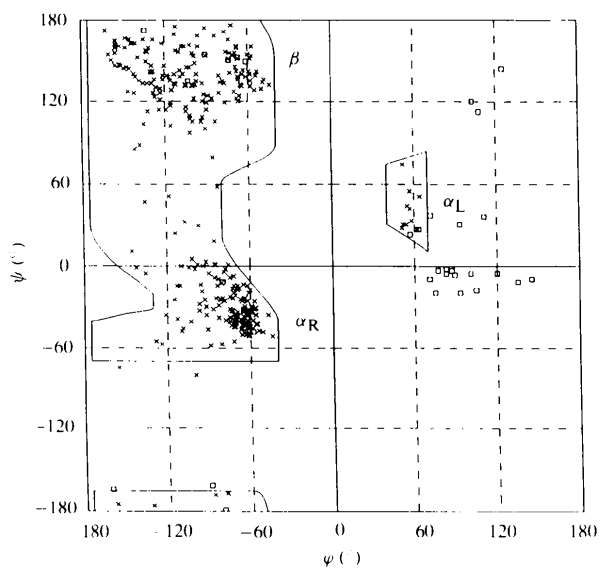

(*b*)

Fig. 2. The Ramachandran plot of the (*a*) *A* and (*b*) *B* subunits of Cu^{II}–LADH–NADH–DMSO complex after refinement. A contour map corresponding to the allowed conformations of the polypeptide backbone is superimposed on the plot. The (○) denotes glycines and crosses denote all other residues.

Results and discussion

The overall structure of Cu^{II}*–LADH*

The r.m.s. differences for backbone and side-chain atoms of Zn^{II}– and Cu–LADH *versus* residue number are presented in Figs. 3(*a*), 3(*b*), 3(*c*) and 3(*d*) for the *A* and *B* subunits. The values for residues with undefined positions of side-chain atoms in the native and Cu^{II}-substituted structures were reset to the average. Only CA atoms were used in the superposition. The mean r.m.s. values for main-chain and side-chain atoms were 0.26 and 0.63 Å, respectively. No changes in the overall structure of the enzyme could be observed, which means that the closed conformation of LADH is identical in the two crystal systems P_1 and $P2_1$. Also the position of the non-catalytic Zn^{II} ion relative to its ligands and its coordination geometry have been preserved. The conformation of NADH is identical in the two structures and described in detail in Al-Karadaghi *et al.* (1994).

It is seen from Fig. 3 that there are a few regions with notable deviations of the r.m.s. values from the average. Some of these residues had poor electron density and their conformations could not be defined unambiguously. In some other cases the high r.m.s. values seem to be caused by differences in crystal-packing contacts. Thus, high values are observed for backbone and side-chain atoms at the N-terminal region of the *A* subunit, particularly for residues 22–29 and 130–140 (about 0.5–0.6 Å for backbone-atom positions). Residues 132–135 constitute a turn between strands 3 and 4 (residues 129–131 and 135–138) of sheet β-III. This turn in the *A* subunit is at close contact with the same region in the *B* subunit of a symmetry-related dimer. Residues 22–29 do not make any direct crystal contacts. The observed distortions in this region seem to be caused by hydrogen-bonding interactions within residues 130–140, which are involved in crystal contacts with the adjacent molecule (O129···N29, N131···O27, O131···N27, N133 ···H20···O25 and N134···H20···OE227). Additional crystal-packing interactions occur between residues Gln244–Lys248 in the *A* and *B* subunits, and between Lys354 in the *A* subunit and Ser1 from the *B* subunit.

For functionally important residues notable shifts in side-chain positions were observed for the metal ligands Cys46, His67 and Cys174. Also the position of the DMSO molecule with respect to the metal ion has

changed considerably. The shifts observed for other residues in the neighbourhood of the Cu^{II} ion are at the level of the average r.m.s. value. From this observation it can be concluded that the positions of side-chain atoms of the metal ligands and of DMSO could not be influenced by the effects of crystal packing at the surface of the protein. The observed differences could not be caused by the experiment either since the crystallization conditions for both Zn^{II}– and Cu^{II}–LADH complexes were identical with the exception that the Cu^{II}-substituted enzyme was crystallized under nitrogen.

The Cu^{II}*-binding centre*

The active-site metal centre in Cu^{II}–LADH is shown in Fig. 4. An $F_o - F_c$ density map with Cu^{II} and the non-liganding alternating position of the S atom of Cys46 omitted from the calculation is shown superimposed on the model. Strong positive maxima centered at the omitted atoms are seen. Fig. 5 shows the superposition of the catalytic metal sites of the *A* subunit of Zn^{II}– and Cu^{II}–LADH. The superposition was performed using the CA atoms of the catalytic domains of the two models. The most prominent difference between the two models is the shift in the position of the inhibitor DMSO. The distance between the O atoms of DMSO in the Zn^{II}– and Cu^{II}–LADH structures is about 1.0 Å (Fig. 5 and Table 2). Similar to the native enzyme the DMSO O atom is still at hydrogen-bonding distance to the OH group of Ser48 in the *A* subunit of Cu^{II}–LADH (2.92 Å). In the *B* subunit the corresponding distance is 3.30 Å. The mean temperature factor for DMSO in the complex with Cu^{II}–LADH is about twice the value in the Zn^{II}–LADH complex: 44, 39 $Å^2$ and 19, 24 $Å^2$ for *A* and *B* subunits, respectively. This higher value is probably a result of a weaker interaction with the metal ion and the partial occupancy (0.85) of the inhibitor site.

The distances from the metal ion to the DMSO O atoms are shown in Table 2 for the native and Cu^{II}-substituted enzymes. For the copper ion the values are about 1 Å longer than the corresponding values for the zinc. This implies only weak interactions between the O atom and Cu^{II}. Nevertheless, these interactions seem to be sufficient to perturb the spectrum of the Cu–LADH–NADH complex. Thus, for the crystals used in this study an absorption maximum of 665 nm was observed with an almost tenfold loss in intensity compared to the binary complex of Cu^{II}–LADH–NADH with absorption maximum at 690 nm (Merli, Rossi & Cedergren-Zeppezauer, unpublished results; Maret *et al.*, 1980).

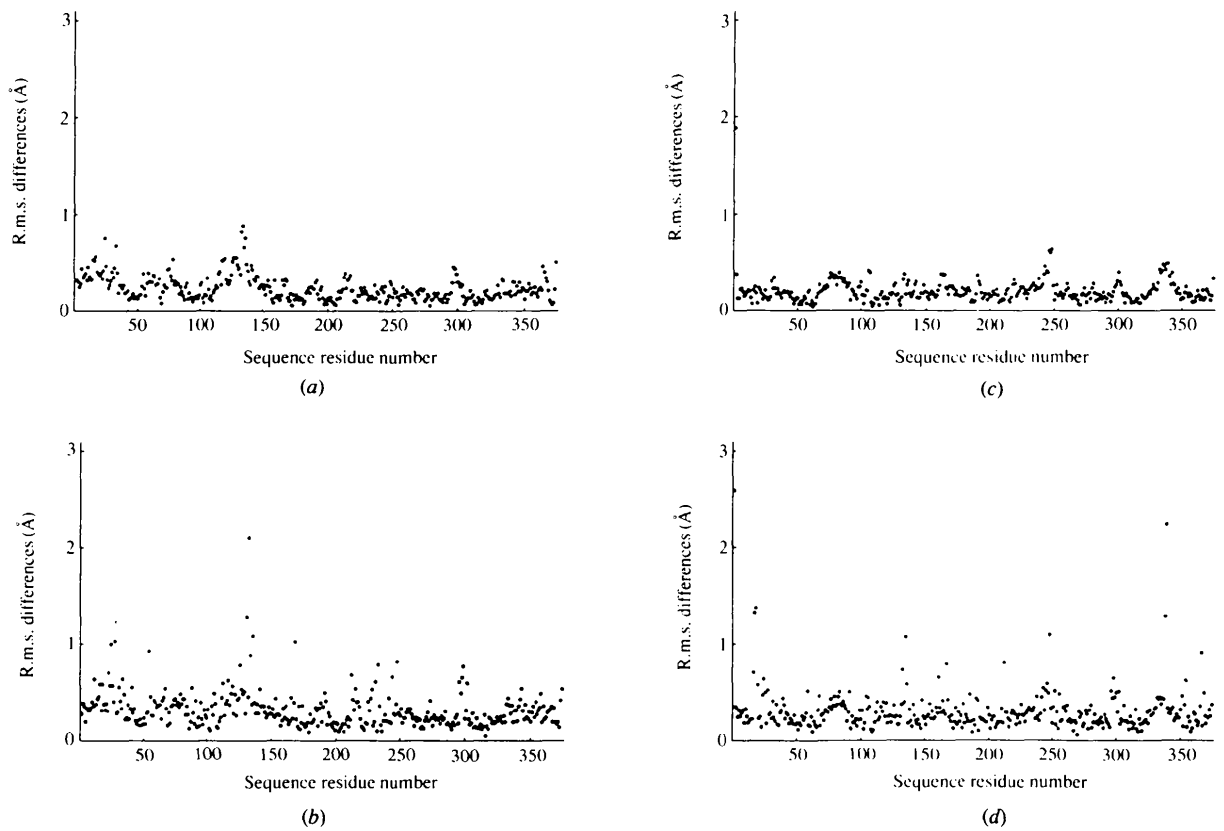

Fig. 3. The r.m.s. difference between the positions of backbone [(*a*) and (*c*)] and side-chain [(*b*) and (*d*)] atoms of the *A* and *B* subunits of Zn^{II}– and Cu^{II}–LADH.

The largest shifts in the relative side-chain positions of the metal ligands are observed for residues His67 and Cys174 (Fig. 5). In the *A* subunit the distance between NE2 of His67 in the two structures is 0.78 Å, between SG of Cys174 it is 0.48 Å and 0.12 Å between the liganding SG atoms of Cys46 (corresponding differences are 0.70, 0.55 and 0.35 Å, for the *B* subunit). Also the Cu^{II} ion is shifted by 0.40 Å relative to the Zn^{II} position in both subunits. The SH group of Cys46 in the second, non-liganding conformation could form a hydrogen bond with OE1 of Glu68 (distance 3.20 Å) which resembles that of metal-depleted apo-LADH (Eklund *et al.*, 1986).

The distances from the protein ligands to the metal ion (Table 2) are rather similar in the Zn^{II} and Cu^{II} enzymes. The $L—Me—L$ (L = ligand, Me = metal) angles (Table 2) are somewhat closer to the tetrahedral value (about 109°) for three of the ligands listed in the case of Zn^{II}, whereas a larger distortion of the tetrahedral geometry is obvious for the Cu^{II} ion. This can also be seen from the comparison of the positions of the Cu^{II} and Zn^{II} ions relative to the plane defined by the two S atoms (Cys46 and Cys174) and the N atom (His67). The Zn^{II} distance to the plane is about twice that of the Cu^{II} (0.32 and 0.18 Å, respectively) (values averaged over the two subunits). Thus, it can be concluded that the coordination of the Cu^{II} ion tends towards a trigonal planar or trigonal pyramidal.

The identity of the methods employed in the refinement of the native Zn^{II}–LADH and the Cu^{II}-substituted complexes allows an estimation of the accuracy of metal–ligand distances and angles to be carried out. This can be obtained from a comparison of the corresponding parameters for the non-catalytic Zn atom in the four subunits of the two models (Table 3). The comparison reveals an average standard deviation for bond lengths and angles of about 0.03 Å and 2°, respectively.

Table 2. *Comparison of metal–ligand distances and angles in the active sites of* Zn^{II}*–LADH–NADH–DMSO and the* Cu^{II}*-substituted complexes*

The values shown are for both subunits of the dimer (*A* and *B*).

	Zn		Cu	
	A	*B*	*A*	*B*
Distance (Å)				
SG46	2.23	2.20	2.34	2.22
NE67	2.15	2.04	2.05	2.16
SG174	2.32	2.26	2.15	2.22
O(DMSO)	2.26	2.13	3.45	3.19
Angles (°)				
SG46—Me—NE67	114	112	110	117
SG46—Me—SG174	130	130	120	129
NE67—Me—SG174	105	108	130	110
SG46—Me—DMSO	105	103	101	119
SG174—Me—DMSO	103	102	95	93
NE67—Me—DMSO	93	94	68	72

Table 3. *Metal–ligand distances and angles for the non-catalytic zinc site in* Zn^{II}*–LADH–NADH–DMSO and the* Cu^{II}*-substituted complex*

The standard deviation from the mean for the respective parameters are in parentheses. *A* and *B* are the different subunits of the enzyme.

	Zn^{II}–LADH		Cu^{II}–LADH		Mean value
	A	*B*	*A*	*B*	
Distances (Å)					
SG97	2.40	2.41	2.46	2.46	2.43 (0.03)
SG100	2.33	2.34	2.35	2.30	2.33 (0.02)
SG103	2.26	2.30	2.21	2.24	2.25 (0.04)
SG111	2.34	2.39	2.36	2.34	2.36 (0.02)
Angles (°)					
SG97—Zn—SG100	107	106	111	109	108 (2)
SG97—Zn—SG103	113	117	115	115	115 (2)
SG97—Zn—SG111	102	104	102	101	102 (2)
SG100—Zn—SG103	107	106	110	108	107 (2)
SG100—Zn—SG111	119	118	116	119	118 (2)
SG103—Zn—SG111	109	107	103	105	106 (3)

Fig. 4. The active site of Cu^{II}–LADH. A difference electron-density map at the 3.5σ level with the Cu^{II} ion and the non-liganding position of Cys46 S atom removed from the model is shown. The position of the copper is marked by a filled circle and the second position of the S atom by SgII. The secondary-structure elements to which the metal-chelating residues belong are also shown.

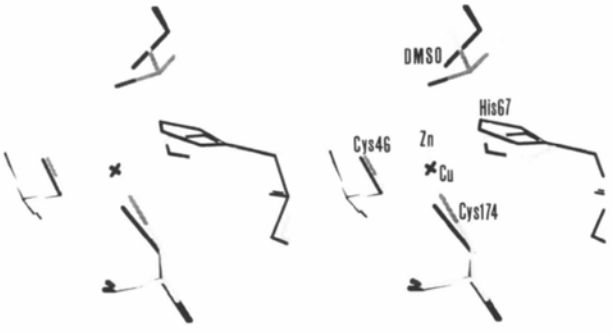

Fig. 5. Stereo plot showing the superposition of the active sites of the Zn^{II}– and Cu^{II}–LADH (grey and black lines, respectively). The displacements of the side chains of His67 and Cys174 and the inhibitor DMSO are seen clearly.

Table 4. *Metal–cysteine dihedral angles in* Zn^{II}– *and* Cu^{II}–*LADH–NADH–DMSO complexes*

	N—CA—CB—SG (°)		CA—CB—SG—Me (°)	
	Cys46	Cys174	Cys46	Cys174
Zn–LADH				
A subunit	172	−178	−179	−167
B subunit	168	−177	−180	−169
Cu–LADH				
A subunit	171	172	−176	−177
B subunit	170	179	−177	−166

Concluding remarks

There are several conserved features in the structure of the copper centre in blue-copper proteins. Chakrabarti (1989) and Han *et al.* (1991) demonstrated the close similarity of the values of sulfur–ligand distances and the torsion angles CA—CB—SG—Cu and N—CA—CB—SG in blue-copper proteins. Also the hydrogen-bonding network around the Cu^{II} ion seems to be preserved (Inoue *et al.*, 1994). A comparison of the coordination environment in Cu^{II}–LADH–NADH–DMSO complex with that of cupredoxins reveals some striking similarities. Thus, the position of the metal with respect to the plane defined by the three strong ligands (Cys112, His46 and His117 in azurin) is similar in Cu^{II}–LADH and azurin: 0.18 and 0.13 Å, respectively. The copper distance to the carbonyl O atom of Gly45 in azurin (3.17 Å) also resembles the observed Cu^{II}–O distance in the complex of LADH with DMSO (3.19 and 3.45 Å). Table 4 presents the values of the torsion angles CA—CB—SG—Cu and N—CA—CB—SG for both cysteine ligands 46 and 174 in the two subunits of Cu^{II}–LADH. The same parameters for the native Zn^{II}–LADH are also presented for comparison. The values of CA—CB—SG—Cu torsion angles averaged over the two subunits of the enzyme are −176.5 and 171.5° for Cys46 and Cys174, respectively. Thus, this angle for Cys174 seems to be closer to the average (about 170°) observed for cupredoxins. However, it is difficult to decide on the basis of the present model only, which of the bonds is responsible for the spectroscopic properties of Cu–LADH.

The variations in metal–ligand bond parameters and in the distance from the metal to the DMSO O atom in the two subunits are larger than the estimated experimental error. Some variations in the same parameters were also observed in the ternary complex of Zn^{II}–LADH–NADH–DMSO, refined at higher resolution. These differences together with the observed shifts in the positions of the protein metal-liganding groups (SG from Cys46 and Cys174 and NE2 from His67) in Cu^{II}–LADH and the native enzyme show that the metal-binding site possesses some degree of flexibility and is not solely a rigid framework for the accommodation of a metal ion. The shifts observed in the metal-depleted enzyme point towards the same conclusion (Eklund *et al.*, 1986).

Similar distortions in the metal-binding site were observed after the substitution of the Cu^{II} ion in azurin by Cd^{II} and Zn^{II} (Nar *et al.*, 1992; Blackwell, Anderson & Baker, 1994; Sjöin *et al.*, 1993). The metal-coordination geometry changed from trigonal bipyramidal in copper azurin to distorted tetrahedral in the zinc protein. This was achieved by rearrangements in the polypeptide backbone which reduced the distance from the Zn^{II} to the carbonyl O atom of Gly45 to 2.36 Å from 2.97 Å for the native Cu^{II} azurin. These changes apparently reflect the need for a mutual adaptation of the positions of the protein ligands and the metal to meet the requirements of the electronic configuration of the metal ion (Vedani & Huhta, 1990). In the case of LADH this limited flexibility of the metal-binding site might be utilized by the enzyme during the catalytic cycle (Tapia *et al.*, 1991).

Dr Hans-Werner Adolph is acknowledged for providing metal-depleted LADH, which was used in the crystallization and Dr K. Petratos for assistance at the EMBL outstation at DESY during an early stage of this work. This work was supported by the Swedish Natural Science Research Council (NFR).

References

ADMAN, E. T., TURLEY, S., BRAMSON, R., PETRATOS, K., BANNER, D., TSERNOGLOU, D., BEPPU, T. & WATANABE, H. (1989). *J. Biol. Chem.* **264**, 87–99.

AL-KARADAGHI, S., CEDERGREN-ZEPPEZAUER, E., PETRATOS, K., HOVMÖLLER, S., TERRY, H. & WILSON, K. (1994). *Acta Cryst.* D**50**, 793–807.

BAKER, E. N. (1988). *J. Mol. Biol.* **203**, 1071–1095.

BLACKWELL, K. A., ANDERSON, B. F. & BAKER, E. N. (1994). *Acta Cryst.* D**50**, 263–270.

BRÄNDÉN, C.-I., JÖRNVALL, H., EKLUND, H. & FURUGREN, B. (1975). *The Enzymes*, Vol. 11, edited by P. D. BOYER, pp. 103–190. New York: Academic Press.

BRÜNGER, A. (1990). *Acta Cryst.* A**46**, 46–57.

BRÜNGER, A. T., KARPLUS, M. & PETSKO, G. A. (1989). *Acta Cryst.* A**45**, 50–61.

CEDERGREN-ZEPPEZAUER, E., SAMAMA, J.-P. & EKLUND, H. (1982). *Biochemistry*, **21**, 4895–4908.

CHAKRABARTI, P. (1989). *Biochemistry*, **28**, 6081–6085.

COLLABORATIVE COMPUTATIONAL PROJECT, NUMBER 4 (1994). *Acta Cryst.* D**50**, 760–763.

DUNN, M. F., DIETRICH, H., MACGIBBON, A. K. H., KOERBER, S. C. & ZEPPEZAUER, M. (1982). *Biochemistry*, **21**, 354–363.

EKLUND, H., JONES, T. A. & SCHNEIDER, G. (1986). *Zinc Enzymes*, edited by I. BERTINI, C. LUCHINAT, W. MARET & M. ZEPPEZAUER, pp. 377–392. Boston: Birkhäuser.

EKLUND, H., NORDSTRÖM, B., ZEPPEZAUER, E., SÖDERLUND, G., OHLSSON, I., BOIWE, T., SÖDERBERG, B.-O., TAPIA, O., BRÄNDÉN, C.-I. & ÅKESON, Å. (1976). *J. Mol. Biol.* **102**, 27–59.

EKLUND, H., PLAPP, B. V., SAMAMA, J.-P. & BRÄNDÉN, C.-I. (1982). *J. Biol. Chem.* **257**, 14349–14358.

EKLUND, H., SAMAMA, J.-P., WALLEN, L., BRÄNDÉN, C.-I., ÅKESON, Å. & JONES, T. A. (1981). *J. Mol. Biol.* **146**, 561–587.

FRENCH, S. & WILSON, K. S. (1978). *Acta Cryst.* A**34**, 517–525.

GUSS, J. M., BARTUNIK, H. D. & FREEMAN, H. C. (1992). *Acta Cryst.* B**48**, 790–811.

GUSS, J. M. & FREEMAN, H. C. (1983). *J. Mol. Biol.* **169**, 521–563.

GUSS, J. M., MERRIT, E. A., PHIZACKERLEY, R. P., HEDMAN, B., MURATA, M., HODGSON, K. O. & FREEMAN, H. C. (1988). *Science*, **241**, 806–811.

HAN, J., ADMAN, E. T., BEPPU, T., CODD, R., FREEMAN, H. C., HUQ, L., LOEHR, T. M. & SANDERS-LOEHR, J. (1991). *Biochemistry*, **30**, 10904–10913.

INOUE, T., KAI, Y., HARADA, S., KASAI, N., OHSHIRO, Y., SUZUKI, S., KOHZUMA, T. & TOBARI, J. (1994). *Acta Cryst.* D**50**, 317–328.

JONES, T. A. (1978). *J. Appl. Cryst.* **11**, 268–272.

LESLIE, A. G., BRICK, P. & WONACOTT, A. J. (1986). *CCP4 Newslett.* **18**, 33–39.

MARET, W., DIETRICH, H., RUF, H.-H. & ZEPPEZAUER, M. (1980). *J. Inorg. Biochem.* **12**, 241–252.

MARET, W. & KOZLOWSKI, H. (1987). *Biochim. Biophys. Acta*, **912**, 329–337.

MARET, W., SHIEMKE, A. K., WHEELER, W. D., LOEHR, T. M. & SANDERS-LOEHR, J. (1986). *J. Am. Chem. Soc.* **108**, 6351–6359.

MARET, W., ZEPPEZAUER, M., DESIDERI, A., MORPURGO, L. & ROTILIO, G. (1981). *FEBS Lett.* **136**, 72–74.

MARET, W., ZEPPEZAUER, M., DESIDERI, A., MORPURGO, L. & ROTILIO, G. (1983). *Biochim. Biophys. Acta*, **743**, 200–206.

MARET, W., ZEPPEZAUER, M., SANDERS-LOEHR, J. & LOEHR, T. M. (1983). *Biochemistry*, **22**, 3202–3206.

NAR, H., HUBER, R., MESSERSCHMIDT, A., FILIPPOU, A. C., BARTH, M., JAQUINOD, M., VAN DE KAMP, M. & CANTERS, G. W. (1992). *Eur. J. Biochem.* **205**, 1123–1129.

PETRATOS, K., DAUTER, Z. & WILSON, K. S. (1988). *Acta Cryst.* B**44**, 628–636.

RAMACHANDRAN, G. N. & SASISEKHARAN, V. (1968). *Adv. Protein Chem.* **23**, 283–437.

READ, R. J. (1986). *Acta Cryst.* A**42**, 140–149.

ROSSMANN, M. & BLOW, D. M. (1962). *Acta Cryst.* **15**, 24–31.

SCHNEIDER, G., CEDERGREN-ZEPPEZAUER, E., KNIGHT, S., EKLUND, H. & ZEPPEZAUER, M. (1985). *Biochemistry*, **24**, 7503–7510.

SCHNEIDER, G., EKLUND, H., CEDERGREN-ZEPPEZAUER, E. & ZEPPEZAUER, M. (1983). *Proc. Natl Acad. Sci. USA*, **80**, 5289–5293.

SJÖLIN, L., TSAI, L.-C., LANGER, V., PASCHER, T., KARLSSON, G. & NORDLING, M. (1993). *Acta Cryst.* D**49**, 449–457.

TAPIA, O., CARDENAS, R., ANDRES, J., KRECHL, M., CAMPILLO, M. & COLONNA-CESASI, F. (1991). *Int. J. Quantum Chem.* **39**, 767–786.

THEORELL, H. & CHANCE, B. (1951). *Acta Chem. Scand.* **5**, 1127–1144.

VEDANI, A. & HUHTA, D. W. (1990). *J. Am. Chem. Soc.* **112**, 4759–4767.